Available online at www.sciencedirect.com

Journal of Catalysis 217 (2003) 233–239

JOURNAL OF CATALYSIS

www.elsevier.com/locate/jcat

Determination of kinetic parameters for the water–gas shift reaction on copper catalysts under realistic conditions for fuel cell applications

N.A. Koryabkina,[a] A.A. Phatak,[a] W.F. Ruettinger,[b] R.J. Farrauto,[b] and F.H. Ribeiro [a,*,1]

[a] *Worcester Polytechnic Institute, Department of Chemical Engineering, 100 Institute Road, Worcester, MA 01609-2280, USA*
[b] *Engelhard Corporation, 101 Wood Avenue, Iselin, NJ 08830, USA*

Received 4 November 2002; revised 23 January 2003; accepted 30 January 2003

Abstract

The kinetic parameters for water–gas shift reaction on Cu-based catalysts were measured under fuel reformer conditions for fuel cell applications (7% CO, 8.5% CO_2, 22% H_2O, 37% H_2, and 25% Ar) at 1 atm total pressure and temperature in the range of 200 °C. The rate per unit of Cu surface area at the stated concentrations was 0.8×10^{-6} mol m^{-2} s^{-1} at 200 °C. The overall reaction rate as a function of the forward rate (r_f) is $r = r_f(1 - \beta)$, where $r_f = k_f[CO]^{0.8}[H_2O]^{0.8}[CO_2]^{-0.7}[H_2]^{-0.8}$, k_f is the forward rate constant, $\beta = ([CO_2][H_2])/(K[CO][H_2O])$ is the approach to equilibrium, and K is the equilibrium constant for the water–gas shift reaction. This expression indicates a strong inhibition on the forward rate by H_2 and CO_2. When ceria was added to the catalyst, it decreased the Cu surface area and did not increase the rate per unit of Cu surface area, suggesting that ceria is not a promoter. The addition of ZnO did not increase the rate per unit of Cu surface area either. Thus, Cu is the active site for catalysis. It was proposed that the kinetics can be explained based on the “Redox” mechanism with $CO* + O* \rightleftarrows CO_2* + *$ as the rate-determining step.

Keywords: Water–gas shift (WGS) reaction on Cu; Rate; Reaction order; Kinetics; Effect of ceria

---

1. Introduction

The water–gas shift (WGS) reaction ($CO + H_2O = CO_2 + H_2$) is used in industrial hydrogen production as well as in fuel processing for fuel cell applications. Its purpose is to produce hydrogen and to reduce the level of CO for final cleanup by preferential oxidation. The WGS reactor currently represents the largest volume of any catalyst in a fuel processor due to the slow kinetics at temperatures where the equilibrium is favorable. The two most studied systems currently are Cu- and Pt-based catalysts. Gas compositions and operating conditions for the WGS reaction can differ significantly between industrial and fuel cell-related applications. One particular problem is that the concentration of the products, H_2 and CO_2, during the WGS reaction is significant in fuel cell applications but many kinetic studies in the literature are carried out without them. This is a severe limitation since we will show in this study that the overall and forward reactions are inhibited by H_2 and CO_2 and thus the rates reported so far tend to be higher than the values at the conditions of interest.

Although the WGS reaction involves only four small molecules, the reaction mechanism is quite complex. There are generally two reaction mechanisms proposed in the literature for the WGS reaction, Associative and Redox. In the first one a formate species is formed which then decomposes forming CO_2 and H_2 [1–3]. The Redox mechanism consists of a surface oxidation, $H_2O + * \rightleftarrows H_2 + O*$, followed by surface reduction, $CO + O* \rightleftarrows CO_2 + *$. Under the conditions of this study it is predicted that the Redox mechanism is probably prevalent [4–7]. Grenoble et al. [2] proposed a reaction sequence based on an associative mechanism including formic acid as an intermediate in order to account for the apparent bifunctionality of the supported catalyst systems. They conclude that the WGS reaction occurs in two sites with the metal activating carbon monoxide and the support sites as the principal sites for water activation. The investigations were carried out using only water and carbon monoxide in the gas stream (20% CO and 30% H_2O). Salmi et al. [3]

---

[*] Corresponding author.
E-mail address: fabio@purdue.edu (F.H. Ribeiro).

[1] Present address: School of Chemical Engineering, Purdue University, 480 Stadium Mall Drive, West Lafayette, IN 47907-2100, USA.

0021-9517/03/$ – see front matter © 2003 Elsevier Science (USA). All rights reserved.
doi:10.1016/S0021-9517(03)00050-2

studied the low temperature water–gas shift reaction on industrial CuO–ZnO catalysts at 200 and 250 °C. They found that the power rate law expression changed when the temperature of reaction was varied, indicating the complex nature of the WGS reaction mechanism. Although the objective of this study was not to study the reaction mechanism, we showed that the Redox mechanism explains our data satisfactorily.

The objective of this study was to determine rates, reaction orders, activation energies, and a kinetic mechanism from experiments conducted under conditions close to the ones likely to be encountered in fuel processors for fuel cell applications on Cu-based catalysts.

2. Experimental methods

The catalysts were prepared by incipient wetness impregnation of the solid support with the nitrates of the corresponding metal, followed by drying at 120 °C (8 h) and calcination at 500 °C (4 h) in air. The alumina support was DD-443 from Alcoa (320 $m^2\,g^{-1}$). The ceria powder was a high surface area ceria ($> 99\%$) $\sim$180 $m^2\,g^{-1}$ from Rhodia. The commercial 40% $CuO–ZnO–Al_2O_3$ catalyst was from United Catalysts. The textural properties for the calcined Alcoa support and for two of the catalysts are listed in Table 1.

The catalysts were reduced by increasing the temperature from 200 to 285 °C at 10 °C min^{-1} and then keeping it at 285 °C for 30 min with a 25% H_2 in Ar mixture. The commercial 40% $CuO–ZnO–Al_2O_3$ catalyst was reduced using a special procedure to avoid exotherms: a 5% H_2 in Ar mixture was used with the temperature increasing from 150 to 200 °C at 0.17 °C min^{-1} and keeping it at 200 °C for 1 h. When the catalysts were present in the pellet form, they were ground to a 45 to 60 mesh fraction. The actual amount of catalyst used was dependent on its activity and was around 0.2 g.

The kinetic measurements were conducted at ambient pressure, temperature range 180–240 °C in a well-mixed continuous-stirred tank reactor (CSTR). A circulation pump (Senior Flexonics Model MB-21HT) with a nominal air flow of 2000 ml min^{-1} was used for the mixing. The entire setup was housed in a forced-air circulation oven maintained at 130 °C. The total inlet flow was 118 ml min^{-1}, with an average inlet gas composition of 7% CO, 8.5% CO_2, 22% H_2O, 37% H_2, and 25% Ar. Argon was used as an internal standard. The gases were fed to the reactor by mass flow controllers. Deionized water was metered by a water pum (Fluid Metering, Inc., Model QVG50) and was vaporized before entering the reactor loop. To avoid fluctuations in the water partial pressure, a 1.6 mm (0.0625 inch) diameter tube capillary with internal diameter 0.254 mm was used to deliver the water. Carbon monoxide was purified by passing it over Cu wire at 320 °C. Carbon dioxide was used without further pretreatment and H_2 passed through a Deoxo trap to remove O_2. The gas stream was continuously analyzed by a mass spectrometer SRS RGA 200 and injected periodically in a gas chromatograph HP5890 equipped with a TCD detector and a Carboxen 1000 column. Before the gases entered the gas chromatograph, a condenser chilled the gases to 0 °C to maintain a low and constant amount of water. Rates were calculated from the CO and CO_2 concentrations and the mass balance on carbon was better than 1%. In all cases the rates were stable and reproducible.

Table 1
Textural properties for selected catalysts and support

Sample	Textural properties		
	S_{BET} ($m^2\,g^{-1}$)	Pore volume ($cm^3\,g^{-1}$)	Average pore radius (nm)
Al_2O_3	230	0.43	3.8
8% $CuO–Al_2O_3$	195	0.36	2.9
8% CuO–15% $CeO_2–Al_2O_3$	170	0.28	2.8

The well-mixed differential reactor used for the measurements minimizes heat and mass transfer limitations by the high circulation rates and also makes the kinetic analysis much simpler since the reactor is differential. We worked in the region where the Arrhenius plot was linear and before transport limitations could be observed by a change in slope. In general, to determine the reaction order of a compound its concentration was varied while the concentrations of the other components were kept constant. The total flow rate was kept constant by adjusting the Ar flow rate. Note, however, that because we worked in the concentration range where the concentrations of reactants and products were significant, we could not keep concentrations constant by using large excess of all compounds. Thus, when the order of a reactant was determined by varying its concentration, the concentration of the remaining reactants could not be kept constant (see Appendix A for one example of the data). An iterative fitting correction was applied to the data to calculate reaction orders.

Copper surface area measurement was carried out by the well-established method of N_2O chemisorption [8], at 60 °C in the same setup used for reaction. The same amount of catalyst as in the kinetic experiments was used. Catalysts were reduced in 5% H_2 and Ar flow by increasing the temperature from 200 to 285 °C at 10 °C min^{-1} and holding the temperature at the maximum value for 30 min. The 40% $CuO–ZnO–Al_2O_3$ catalyst was reduced using the same parameters except that the temperature varied from 160 to 235 °C. The catalyst was then flushed in Ar for at least 2 h and kept isolated until the 3% N_2O flow in Ar (50 ml min^{-1}) was stabilized. Finally, the flow was directed to the catalyst and the N_2 signal from the reaction $N_2O + Cu \rightarrow N_2 + Cu_2O$ was monitored by MS as a measure of the uptake. The amount of N_2 was calculated by injecting a calibrated pulse amount of N_2 into the stream. A density of 1.8×10^{19} Cu atoms m^{-2} was used for the area calculation. This is the density of atoms on a Cu(111) plane which we assume as the dominating surface structure on the catalyst particles. The uptake of N_2O to measure Cu surface area could not be

Table 2
Rates of reaction for the overall WGS reaction on Cu-based catalysts at 200 °C, 1 atm total pressure, 7% CO, 8.5% CO_2, 22% H_2O, 37% H_2, and 25% Ar

	Catalysts				
	8% CuO–CeO_2	8% CuO–15% CeO_2–Al_2O_3	8% CuO–Al_2O_3	12% CuO–Al_2O_3	40% CuO–ZnO–Al_2O_3
Rate per gram of catalyst (10^{-6} mol g^{-1} s^{-1})	0.11	0.75	2.4	4.0	7.6
Rate per mol of Cu (10^{-4} mol mol^{-1} s^{-1})	1.1	7.5	23	26	20
Rate per area of Cu (10^{-6} mol m^{-2} s^{-1})	–	0.83	0.80	0.78	0.79
Cu surface area (m^2 g^{-1})	–	0.9	3.0	5.1	9.6

used on ceria-containing catalysts as ceria is reduced during treatment in H_2 and it reacts with N_2O to form N_2. The Cu area was measured instead from the uptake of CO following N_2O oxidation. This method is based on the finding by Dandekar and Vannice [9] that CO will adsorb strongly on Cu^+. It also assumes that CO will not adsorb strongly on ceria after oxidation by N_2O. The procedure consisted of measuring the N_2O uptake as described above. After flushing the system with Ar, the temperature was decreased to 30 °C and a flow of 5% CO in Ar was started. The amount of CO adsorbed was calculated by measuring the CO concentration with the MS. A second CO uptake, after flushing with Ar at 30 °C, was used to measure reversible chemisorption. The difference between the two CO uptakes was used as a measure of irreversibly adsorbed CO. This second method did not work for the ceria-supported sample (8% CuO–CeO_2); the pure ceria support had probably some residual activity and the measured area was unreasonably high.

We have estimated the accuracy of the measurements by carrying out multiple experiments. For the rates per gram of catalyst there were differences in rates of about 20%. We suspect they were due mostly to nonuniformities on the metal distribution in the pellets. The apparent activation energies could be reproduced with better than 5% and the reaction orders within 10%.

3. Results

The reaction rates are reported in Table 2 per unit of mass of catalyst, per mole of total Cu, and per unit of Cu surface area. On the basis of unit of mass of catalyst, the industrial CuO–ZnO–Al_2O_3 catalyst is the most active. The rate per mole of Cu does not change appreciably as the Cu concentration is varied from 8 to 30% when ceria is not present. The ceria-containing catalysts have lower rates per unit of mass and lower Cu surface area. The rate per unit of Cu surface area is constant on all samples. Note that the turnover rates were compared at 200 °C but because the activation energies are not identical (Table 3), the agreement among the turnover rates on the various catalysts will be less perfect at other temperatures. The temperature of 200 °C was chosen for the comparison because it was the temperature closest to the actual one used in the measurements for the catalysts in Table 2.

Table 3
Apparent activation energy and power-rate law reaction order for the forward WGS reaction on Cu-based catalysts

Catalyst	E_a	Temperature[a]	Reaction order			
	(kJ mol^{-1})	(°C)	CO[b]	H_2O[c]	CO_2[d]	H_2[e]
8% CuO–Al_2O_3	62	200	0.9	0.8	−0.7	−0.8
8% CuO–15% CeO_2–Al_2O_3	32	200	0.7	0.6	−0.6	−0.6
8% CuO–CeO_2	56	240	0.9	0.4	−0.6	−0.6
40% CuO–ZnO–Al_2O_3	79	190	0.8	0.8	−0.9	−0.9

[a] Temperature at which the reaction order measurements were carried out.

[b] Concentration range: 5 to 25% CO and balance Ar to 33%; 8.5% CO_2, 22% H_2O, 37% H_2.

[c] Concentration range: 10 to 46% H_2O and balance Ar to 47.5%; 7% CO, 8.5% CO_2, 37% H_2.

[d] Concentration range: 5 to 30% CO_2 and balance Ar to 34%; 7% CO, 22% H_2O, 37% H_2.

[e] Concentration range: 25 to 60% H_2 and balance Ar to 62.5%; 7% CO, 8.5% CO_2, 22% H_2O.

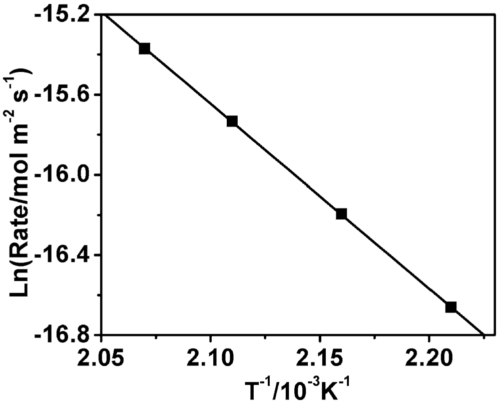

Fig. 1. Arrhenius plot for the WGS reaction on 40% CuO–ZnO–Al_2O_3 at 1 atm total pressure. Rates per unit of Cu surface area were corrected for the conditions 7% CO, 8.5% CO_2, 22% H_2O, 37% H_2, and 25% Ar.

The experimentally determined activation energies and reaction orders are presented in Table 3. To illustrate the quality of the kinetic data, the Arrhenius plot (Fig. 1) and reaction orders (Fig. 2) are shown for the 40% CuO–ZnO–Al_2O_3 sample. The complete data set is also given in Appendix A. Apparent activation energies usually do not change considerably for a group of catalysts but the addition of ceria to the alumina-supported catalyst caused

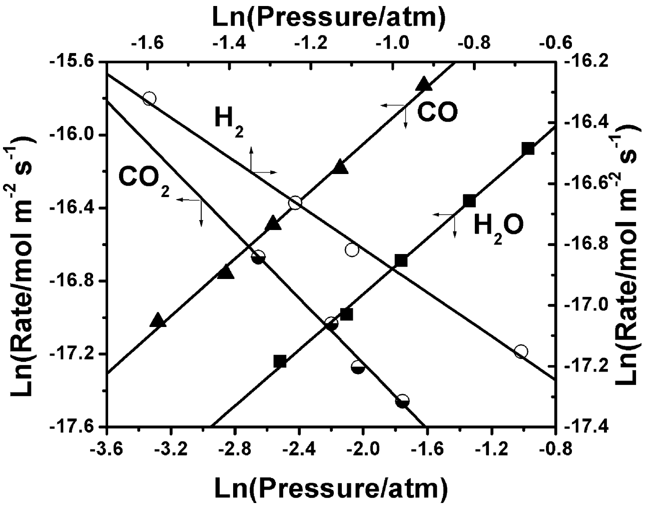

Fig. 2. Determination of power-rate law orders. Rate of the WGS reaction per unit of Cu surface area measured on 40% CuO–ZnO–Al_2O_3 catalysts at 190 °C 1 atm total pressure. Partial pressures for all components reported in Appendix A.

the activation energy to decrease by a factor of 2 while the activation energy was not affected on the Cu catalyst supported on ceria. To determine the reaction orders with respect to reactants and products, the kinetic data were fitted to a power-rate law expression. For clarity, we will describe the derivation of the rate expression with the assumptions made [10,11]. The overall rate will be assumed to be of the form,

$$\text{Rate} = k_\mathrm{f}[\mathrm{CO}]^a[\mathrm{H_2O}]^b[\mathrm{CO_2}]^c[\mathrm{H_2}]^d - k_\mathrm{r}[\mathrm{CO}]^e[\mathrm{H_2O}]^f[\mathrm{CO_2}]^g[\mathrm{H_2}]^h,$$

where k_f is the forward rate constant, a, b, c, and d are forward reaction orders, k_r is the reverse rate constant, and e, f, g, h are reverse reaction orders. If one assumes that the power-rate law expression will be valid at any distance from equilibrium, at equilibrium

$$k_\mathrm{f}/k_\mathrm{r} = [\mathrm{CO}]^{e-a}[\mathrm{H_2O}]^{f-b}[\mathrm{CO_2}]^{g-c}[\mathrm{H_2}]^{h-d} \quad \text{and} \quad K = \big([\mathrm{CO_2}][\mathrm{H_2}]\big)/\big([\mathrm{CO}][\mathrm{H_2O}]\big),$$

where K is the equilibrium constant for the water–gas shift reaction. With this relationship we can write the ratios

$$(e-a)/(-1) = (f-b)/(-1) = (g-c)/1 = (h-d)/1 = 1/n,$$

where n is a constant and thus $K^{1/n} = k_\mathrm{f}/k_\mathrm{r}$. With one more assumption that the value of n is 1,

$$\text{Rate} = k_\mathrm{f}[\mathrm{CO}]^a[\mathrm{H_2O}]^b[\mathrm{CO_2}]^c[\mathrm{H_2}]^d(1-\beta),$$

where $\beta = ([\mathrm{CO_2}][\mathrm{H_2}])/(K[\mathrm{CO}][\mathrm{H_2O}])$ is the approach to equilibrium. Note that this equation can be best rationalized if a reversible rate-determining step with a stoichiometric number of 1 is assumed. The values for β in our experiments were usually of the order of 0.03–0.1, which indicates that the reaction was carried out far from equilibrium. Note that by reporting the value of the overall rate, the forward rate constant and reaction orders for the forward reaction, one can calculate the kinetic parameters for the reverse reaction.

4. Discussion

4.1. Rate of reaction and apparent activation energy

The absence of heat and mass transport limitations in our data can be concluded from the Madon–Boudart test [12] since the 12 and 8% copper catalysts have the same rate per unit of Cu surface area (Table 2). In fact, the rate per unit of Cu surface area is the same for all catalysts tested.

The constancy of rate per unit of Cu surface area in Table 2 indicates that the reaction occurs on Cu only and that ceria and ZnO do not affect the rates. The addition of ceria decreases the amount of available Cu surface area as shown by a lower Cu surface area for the 8% CuO–15% CeO_2–Al_2O_3 catalyst compared to the 8.0% CuO–Al_2O_3 catalyst. The most efficient catalyst on a per weight basis is the industrial one, as this catalyst must have been optimized for maximum rate per unit of volume. Comparison of the rate per total mole of Cu shows that the industrial catalyst and the Cu on alumina samples have about the same rate but that when ceria is added the rate decreases. These results show again that ceria does not promote Cu catalysts under the conditions tested.

Comparison of rates with the ones in the literature is complicated by the fact that most studies were carried out under different conditions and the inhibitory effect of CO_2 and H_2 was not discussed. Not accounting for this inhibition may make the rate evaluated under the conditions prevalent on a reformer for fuel cell applications appear to be much higher. A compilation from the rate data in the literature corrected to our conditions from the data provided in the original papers is shown in Table 4. The rate that was measured closer to our conditions is from Ovesen et al. [7]. Assuming that their reactor behaves as a plug flow and that the correction for the pressure as specified in their paper is $(\text{pressure})^{-0.4}$ gives a rate that is in excellent agreement with the value we report. For the other values in Table 4, various extrapolations and assumptions had to be made for the overall rate calculations. Although the rate data agreement is close in some cases one should keep in mind that they were originally measured under conditions different from ours and without accounting for the effect of inhibition by CO_2 and H_2.

Comparison of activation energies with most of the values reported in the literature was also made but good agreement may not be possible since most studies omitted the inhibitory effects from H_2 and CO_2. This omission will result in the determination of apparent rate constants that will be lower than the actual ones, which in turn result in an apparent activation energy that is lower than the actual one. For example, a reaction order of −1 in the product that is not

Table 4
Literature values for kinetics on WGS reaction

Catalyst	Temperature[a] (°C)	Rate[b] (10^{-6} mol m^{-2} s^{-1})	E_a[c] (kJ mol^{-1})	Reaction order[c] CO	H_2O	CO_2	H_2	Ref.
$CuO/ZnO/Al_2O_3$	190	0.79	79	0.8	0.8	−0.9	−0.9	This work
$CuO/ZnO/Al_2O_3$	180–200	0.91	86	1[d]	1.4	−0.7	−0.9	[7]
10% Cu/Al_2O_3	130	19	55	0.30	0.38	–	–	[2]
CuO/CeO_2	175–300	–	19.2–30.4[e]	0–1[e]	1–0[e]	–	–	[15]
$CuO/ZnO/Al_2O_3$	200	0.75	67	0.2[f]	0.6[f]	0	0	[1]
CuO–ZnO (ICI 52-1)	200	0.14	–	0.45	0.07	–	–	[3]
Cu(111)	340	0.32	71	0	0.5–1	–	–	[13]
Cu(110)	340	14	42	0	1	–	–	[5,14]

[a] Temperature at which the reaction order measurements were carried out.

[b] Rates of reaction per unit of Cu surface area for the overall WGS reaction corrected to 200 °C, 1 atm total pressure, 7% CO, 8.5% CO_2, 22% H_2O, 37% H_2, and 25% Ar.

[c] Apparent activation energy and reaction orders for the forward reaction.

[d] Assumed as first order in [7].

[e] Depending on the CO to H_2O ratio.

[f] Calculated at our conditions from the analytical expression provided.

corrected for inhibition will result in an apparent activation energy that will be half of the actual value. Ovesen et al. [7] accounted for the inhibition and the value they report on the CuO–ZnO catalyst is similar to the one we measured (Table 4). The other values for activation energy in Table 4 did not consider inhibition by CO_2 and H_2 or may have been determined at conditions very different from the ones we studied. The result from Grenoble et al. [2] for 10% Cu/Al_2O_3 in Table 4 is similar to the one we found on Cu/Al_2O_3. There is also our own low value for the 8% CuO–15% CeO_2–Al_2O_3 sample, which is similar to the value on CuO–CeO_2 described by Li et al. [15]. The factor of 2 lower activation energy for the 8% CuO–15% CeO_2–Al_2O_3 sample than the one on the 8% CuO–Al_2O_3 sample might suggest that the sample operated in a regime of severe internal diffusion. This does not seem to be the case since the rate per gram on this catalyst is a factor of 3 lower than on the 8% CuO–Al_2O_3 catalyst, and Table 1 shows that the addition of ceria to the copper catalyst results in a small change in the average pore size radius. The data on the industrial catalyst suggests that addition of ZnO results in an increase in the apparent activation energy.

4.2. Reaction kinetics

A power-rate law expression is very useful for the design of reactors (Table 3). It also serves as an indication of the prevalent reaction mechanism, especially when the expression can be obtained for different samples under the same conditions of temperature and concentration. An inspection of Table 3 reveals that the mechanism may be similar on all catalysts. The differences in reaction orders are not interpreted as a significant difference.

Some of the previous literature results on reaction orders are summarized in Table 4. The comment made above about comparison of our data with the ones in the literature where the inhibiting effect of CO_2 and H_2 was not considered is also valid here. In addition, since the power-rate law may change as temperature and concentration ranges are changed, agreement with our data is expected only if temperature and concentration ranges are similar. Only Ovesen et al. [7] had temperature and partial pressures similar to ours. The power rate law they measured is similar to the one we report. It is not surprising that the other values were different from ours. Thus, the values provided in this paper should be used for rate calculations under fuel cell reformer conditions.

Extracting a plausible reaction mechanism from a power-rate law is possible in many cases [16]. For the water–gas shift reaction, however, as is apparent from the complexity of the power-rate law expression, it is not the case. The inherent complexity of this reaction is further illustrated by the fact that the same Cu catalyst, under different reaction conditions, is also used to produce methanol. The best approach to study the WGS mechanism is a kinetic analysis where the elementary steps are considered with all rate constants and the resulting system of equations is solved simultaneously. This method has been detailed in general for example by Dumesic et al. [17] and for the WGS reaction by Lund [18]. Here we will use the same method and reaction steps as described in Ovesen et al. [6,7] to study our data. Their mechanism can be represented as (where $*$ is a free site) [6]:

$$H_2O + * \rightleftarrows H_2O*, \tag{1}$$

$$H_2O* + * \rightleftarrows OH* + H*, \tag{2}$$

$$2OH* \rightleftarrows H_2O* + O*, \tag{3}$$

$$OH* + * \rightleftarrows O* + H*, \tag{4}$$

$$2H* \rightleftarrows H_2 + 2*, \tag{5}$$

$$CO + * \rightleftarrows CO*, \tag{6}$$

$$CO* + O* \rightleftarrows CO_2* + *, \tag{7}$$

$$CO_2* \rightleftarrows CO_2 + *. \tag{8}$$

The mechanism (1)–(8) can be seen as a surface oxidation, obtained by combining steps (1)–(5), $H_2O + * \rightleftarrows H_2 + O*$, followed by surface reduction, obtained by combining steps (6)–(8), $CO + O* \rightleftarrows CO_2 + *$. For this reason it is called a Redox mechanism. For the calculations Ovesen et al. [6] assumed that: (i) steps (1), (3), (5), (6), and (8) are in equilibrium, (ii) the remaining steps (2), (4), and (7) may not be in equilibrium and could be rate determining, (iii) the catalyst surface is uniform, (iv) the catalyst surface is composed of mostly Cu(111) planes, which implies that the equilibrium constants and rate constants can be directly taken or calculated from published literature data on Cu(111) single crystal studies. From the five equations for the five steps in equilibrium, the equation for the conservation of the total number of surface sites, and the steady-state balance for $O*$ and $OH*$ one obtains seven equations and thus can determine the expression for the coverage of the seven unknowns: the six surface compounds H_2O*, $OH*$, $H*$, $O*$, $CO*$, CO_2* and the number of free sites ($*$). The rate of reaction can then be written as an algebraic expression using the partial pressure of reactants and products and equilibrium and rate constants. The calculated rates using the rate constants and adsorption constants taken from Ovesen et al. [6,7] overestimated our experimental rates and for a better fitting we changed the activation energy for the forward reaction on step (7) from 72.2 to 77.7 $\mathrm{kJ\,mol^{-1}}$; the rates are quite dependent on this value. The fitting is presented in Fig. 3. Note that no adjustable parameters, except for the activation energy in step (7), were used. For finding the rate-determining step (RDS) we used the procedure suggested by Campbell [19,20] of calculating the degree of rate control $\partial \ln(\text{rate})/\partial \ln(\text{rate constant})$ for each step, calculated by keeping all the rate constants for the other steps constant and the equilibrium constant for this step constant. From the possible candidate steps ((2), (4), and (7)) the value of degree of rate control for step (7) is one while the values for (2) and (4) are close to zero, which indicates that step (7) is the RDS. Despite of the good agreement between calculated and measured rates, the mechanism above or its development [7] could not predict the negative reaction order for CO_2, although the other reaction orders are in good agreement. The model also overestimates the calculated overall equilibrium constant at 190 °C by a factor of 2.5. Other models are available in the literature, for example, by Fishtik and Datta [21], although the negative order for CO_2 could not be explained either. The issue of how to modify the mechanism to account for a negative reaction order in CO_2 was addressed in detail by Ovesen et al. [7]. The authors included a step for the synthesis of formate ($CO_2* + H* \rightleftarrows HCOO* + *$) in their model. However, the formate species concentration is predicted [22] to be high under methanol synthesis conditions (50–100 bar) but insignificant at 1 bar [7]. In fact, Ovesen et al. [7] predict a reaction order close to zero at 1 bar even with the formate step. In nonpublished work, we included this step in the mechanism using a full microkinetic analysis with values from Ovesen et al. [23] and also found it could not explain the negative CO_2 order. One explanation for the inability of the kinetic model to predict the apparent reaction order is that the Cu surface reconstructs or changes its surface area under reaction conditions. This model was proposed for the WGS [14] and methanol synthesis reactions [23]. Thus, a better model is necessary to explain the inhibition by CO_2.

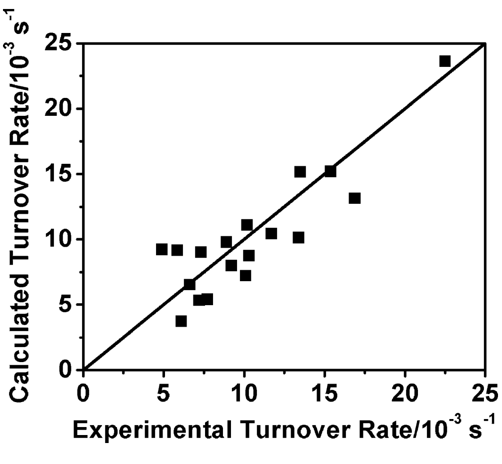

Fig. 3. Comparison of experimental turnover rate to the one calculated using kinetic modeling.

4.3. *Effect of ceria and zinc oxide*

The rate measurements and Cu surface area in Table 2 and reaction orders in Table 3 suggest that when ceria is added to Cu, it reduces the Cu surface area. There is no promotion observed in the WGS reaction, contrary, for example, to the promotion of ceria to Pt or Pd [24]. Li et al. [15] reported promotion on the Cu–ceria. The rate for the catalyst supported on ceria must be compared per mole of total Cu, since the Cu surface area could not be measured precisely in this case due to interference from ceria. Our rate from Table 2 is $1.1 \times 10^{-4}\ \mathrm{mol\,mol^{-1}\,s^{-1}}$, lower than the rate of $14 \times 10^{-4}\ \mathrm{mol\,mol^{-1}\,s^{-1}}$ calculated from the data in Li et al. [15]. Our explanation for this difference is that their reaction conditions were different from the ones used here, especially that the amounts of H_2 and CO_2 they used were low. In our case, the high H_2 partial pressure may reduce the ceria and make it susceptible to reaction with CO_2, which is present in much higher concentration, thus poisoning the ceria.

The addition of ZnO to the industrial catalyst also does not modify the rate per unit of surface area of Cu. It suggests that ZnO does not promote the rate of reaction. This fact was pointed out previously by Campbell and Daube [13] on studies on Cu(111) surfaces.

5. Summary

We report rates of reaction, measured at conditions relevant for production of H_2 for fuel cell application, on

Table A.1
Turnover rate (TOR) at the partial pressures indicated for 40% CuO–ZnO–Al_2O_3 at 190 °C

P_{CO} (atm)	P_{CO_2} (atm)	P_{H_2} (atm)	P_{H_2O} (atm)	P_{Ar} (atm)	TOR (10^{-2} s^{-1})
		CO order data			
0.077	0.093	0.381	0.213	0.237	1.18
0.038	0.090	0.378	0.216	0.280	0.73
0.117	0.095	0.383	0.210	0.195	1.54
0.058	0.091	0.379	0.214	0.258	0.92
0.197	0.100	0.388	0.206	0.110	2.26
0.061	0.092	0.380	0.214	0.254	1.03
		CO_2 order data			
0.065	0.173	0.370	0.217	0.176	0.49
0.061	0.070	0.366	0.214	0.289	1.03
0.064	0.131	0.369	0.216	0.219	0.59
0.063	0.111	0.368	0.216	0.243	0.74
		H_2 order data			
0.059	0.094	0.203	0.211	0.433	1.36
0.061	0.091	0.290	0.214	0.344	1.02
0.063	0.089	0.504	0.216	0.127	0.67
0.062	0.091	0.333	0.214	0.300	0.89
		H_2O order data			
0.064	0.089	0.369	0.081	0.398	0.61
0.057	0.096	0.362	0.379	0.107	1.70
0.063	0.090	0.368	0.122	0.358	0.78
0.059	0.094	0.364	0.262	0.221	1.34
0.061	0.091	0.366	0.171	0.310	1.01

a series of Cu-based catalysts. Strong inhibition by the reaction products (CO_2 and H_2) was observed. Hence, the reaction rates determined under conditions pertinent to fuel cell applications from the rate data in previous studies in the literature might be higher than the ones reported here. This is mostly because most of the previous studies did not consider the inhibition of the forward rate by CO_2 and H_2 under their experimental conditions. Also, the kinetics and conclusions about the reaction mechanism may have been compromised in these studies. At the conditions used in our study, ceria or zinc oxide were not found to have a promoting effect. The rate per unit of Cu surface area was constant on all samples. The results indicate that Cu is the active phase for catalysis. The power-rate law reaction orders were similar for all catalysts. The kinetic modeling supports the surface Redox mechanism with the reduction of surface oxygen by adsorbed CO as the rate-determining step.

Acknowledgment

One of us (FHR) gratefully acknowledges support from the Office of Basic Energy Sciences, Chemical Sciences, US Department of Energy, Grant DE-FG02-00ER15026.

Appendix A

We provide in Table A.1 the data used to derive the reaction orders shown in Fig. 2 and Table 3 for the 40% CuO–ZnO–Al_2O_3 catalyst. The turnover rate is given as a function of partial pressure for all components (CO, CO_2, H_2, H_2O, and Ar) in a well-stirred flow reactor (CSTR). The experiments were carried out at 190 °C, 1 atm total pressure, total flow rate 118 $ml\,min^{-1}$, 0.2 g of catalyst, Cu surface area of 9.6 $m^2\,g^{-1}$. We assumed all Cu particles expose the Cu(111) plane with a density of 1.8×10^{19} $atoms\,m^{-2}$.

References

[1] T. Van Herwijnen, W.A. De Jong, J. Catal. 63 (1980) 83.
[2] D.C. Grenoble, M.M. Estadt, D.F. Ollis, J. Catal. 67 (1981) 90.
[3] T. Salmi, R. Hakkarainen, Appl. Catal. 49 (1989) 285.
[4] G.C. Chinchen, M.S. Spencer, K.C. Waugh, D.A. Whan, J. Chem. Soc., Faraday Trans. 1 83 (1987) 2193.
[5] J. Nakamura, J.M. Campbell, C.T. Campbell, J. Chem. Soc., Faraday Trans. 86 (1990) 2725.
[6] C.V. Ovesen, P. Stoltze, J.K. Nørskov, C.T. Campbell, J. Catal. 134 (1992) 445.
[7] C.V. Ovesen, B.S. Clausen, B.S. Hammershoei, G. Steffensen, T. Askgaard, I. Chorkendorff, J.K. Nørskov, P.B. Rasmussen, P. Stoltze, P. Taylor, J. Catal. 158 (1996) 170.
[8] J.J.F. Scholten, J.A. Konvalinka, Trans. Faraday Soc. 65 (1969) 2465.
[9] A. Dandekar, M.A. Vannice, J. Catal. 178 (1998) 621.
[10] H. Bohlbro, An Investigation on the Kinetics of the Conversion of Carbon Monoxide with Water Vapor over Iron Oxide Based Catalysts, Gjellerup, Copenhagen, 1969.
[11] K. Tamaru, in: Dynamic Heterogeneous Catalysis, Academic Press, New York, 1978, p. 7.
[12] R.J. Madon, M. Boudart, I&EC Fundam. 21 (1982) 438.
[13] C.T. Campbell, K.A. Daube, J. Catal. 104 (1987) 109.
[14] K.H. Ernst, C.T. Campbell, G. Moretti, J. Catal. 134 (1992) 66.
[15] Y. Li, Q. Fu, M. Flytzani-Stephanopoulos, Appl. Catal. B 27 (2000) 179.
[16] M. Boudart, G. Djéga-Mariadassou, Kinetics of Heterogeneous Catalytic Reactions, Princeton Univ. Press, Princeton, NJ, 1984.
[17] J.A. Dumesic, D.F. Rudd, L.M. Aparicio, J.E. Rekoske, A.A. Treviño, The Microkinetics of Heterogeneous Catalysis, Am. Chem. Society, Washington, DC, 1993.
[18] C.R.F. Lund, Ind. Eng. Chem. Res. 35 (1996) 2531.
[19] C.T. Campbell, Topics Catal. 1 (1994) 353.
[20] C.T. Campbell, J. Catal. 204 (2001) 520.
[21] I. Fishtik, R. Datta, Surf. Sci. 512 (2002) 229.
[22] T.S. Askgaard, J.K. Nørskov, C.V. Ovesen, P. Stoltze, J. Catal. 156 (1995) 229.
[23] C.V. Ovesen, B.S. Clausen, J. Schiotz, P. Stoltze, H. Topsoe, J.K. Nørskov, J. Catal. 168 (1997) 133.
[24] T. Bunluesin, R.J. Gorte, G.W. Graham, Appl. Catal. B 15 (1998) 107.